Available online at www.sciencedirect.com
ScienceDirect
Journal of Magnetic Resonance 187 (2007) 205–215
JMR Journal of Magnetic Resonance
www.elsevier.com/locate/jmr

New pulse sequences for recording 2D NMR spectra to analyse mixtures of deuterated *unlike/like* stereoisomers using weakly orienting chiral liquid crystals

Patrick Berdagué [a], Olivier Lafon [b], Hervé Zimmermann [c], Eric Guittet [a], Philippe Lesot [b,*]

[a] *Laboratoire de Chimie et Biologie Structurales, ICSN CNRS UPR 2301, Gif-sur-Yvette 91198, France*
[b] *Laboratoire de Chimie Structurale Organique, RMN en Milieu Orienté, ICMMO CNRS UMR 8182, Bât. 410, Université de Paris-Sud (XI), 91405 Orsay, France*
[c] *Max-Planck-Institut für Medizinische Forschung, Abteilung Biophysik, Jahnstrasse 29, 69120 Heidelberg, Germany*

Received 30 January 2007; revised 6 April 2007
Available online 20 April 2007

Abstract

We describe several new two-dimensional NMR strategies dedicated to the analysis of the isotropic ^{1}H spectra of the mixture of dideuterated *unlike/like* stereoisomers with two vicinal stereogenic centers, using weakly orienting chiral liquid crystals. To this end, we propose various 2D correlation experiments, denoted "J(H,H)" or "J(H,C)" (with $n = 1, 2$), that involve two-dimensional separation of INEPT-type with one or two proton relays. The analytical expressions of correlation signals for four pulse sequences were calculated using the product-operators formalism for $I = 1$ and $S = 1/2$. The features and advantages of each sequence are presented and discussed. The efficiency of these 2D sequences is illustrated using various deuterated model molecules, dissolved in organic solutions of polypeptides made of poly-γ-benzyl-L-glutamate (PBLG) or poly-ε-carbobenzyloxy-L-lysine (PCBLL) and NMR theoretical simulations.

Keywords: ^{1}H quadrupolar splittings; 2D experiments; Chiral liquid crystals; INEPT transfers; Proton relay; *u/l* Stereoisomers

1. Introduction

^{1}H NMR spectroscopy in chiral polypeptide liquid crystals provides original solutions to organic chemistry for analyzing relative stereochemistry of molecules, determining the enantiomeric purity of a mixture, or answering to specific analytical issues [1–4]. Among stereochemical problems met by chemists, the analysis of a mixture made of deuterated *unlike/like* (*u/l*) compounds with two vicinal stereogenic carbons of different stereochemistry for each asymmetric carbon is particularly challenging [5]. For illustration, typical molecules of interest are shown in Fig. 1. In these examples, the *unlike* and *like* isomers correspond to the achiral compound (*meso* form) and the enantiomers (*RR/SS*), respectively.

For such mixtures, the discrimination of diastereoisomeric forms (*u/l*) in isotropic NMR is not always possible, in particular when the stereogenic centers are far from each other [5]. Besides, the discrimination of enantiomers (*RR/SS*) is basically impossible since the NMR solvent is generally achiral. Alternatively, the use of ^{1}H–{^{1}H} or ^{13}C–{^{1}H} NMR spectroscopies in chiral liquid crystals can afford efficient solutions to separate the signals of the three stereoisomeric forms, the achiral isomer (*meso*) and two enantiomers (*RR/SS*), on the basis of quadrupolar splittings or chemical shift anisotropy (CSA) differences [2]. Indeed, the oriented chiral solvent allows to orient differently the average *u/l* diastereoisomers as well as enantiomers of the mixture.

For mixtures **1** or **2**, four distinct quadrupolar doublets are expected to be observed on ^{1}H–{^{1}H} spectra, assuming

* Corresponding author. Fax: +33 (0)1 69 15 81 05.
E-mail address: philesot@icmo.u-psud.fr (P. Lesot).

1090-7807/$ - see front matter © 2007 Elsevier Inc. All rights reserved.
doi:10.1016/j.jmr.2007.04.007

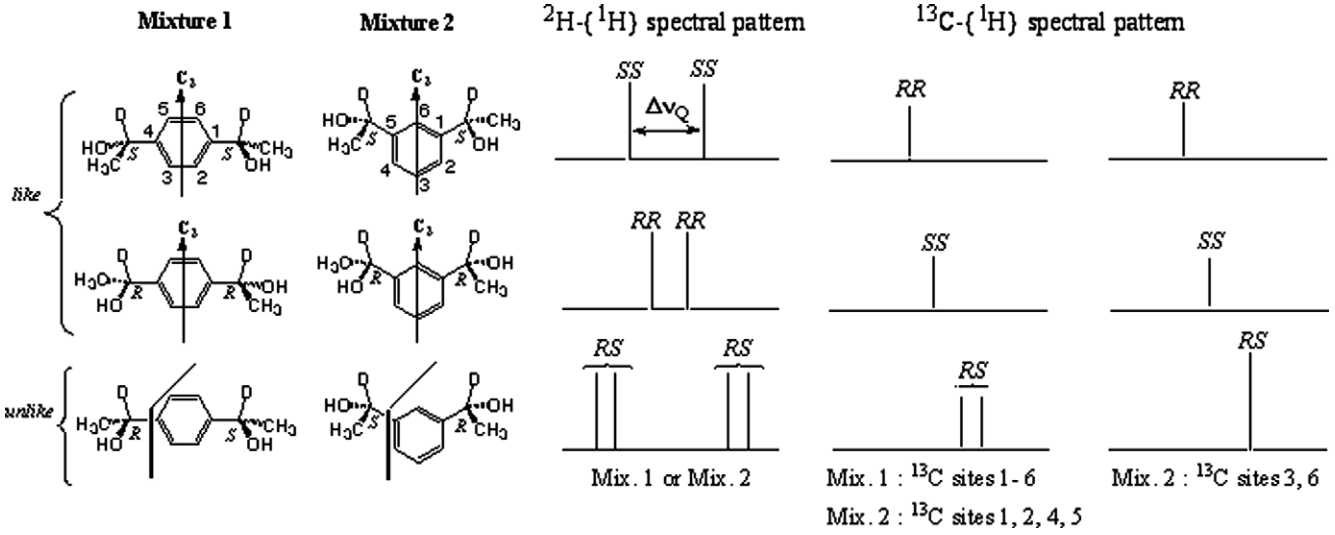

Fig. 1. Schematic ^{2}H–{^{1}H} and ^{13}C–{^{1}H} NMR spectral patterns expected to be observed for various isomeric mixtures **1** and **2** dissolved in a chiral lyotropic nematic phase when all coupling constants are spectrally discriminated. Due to the C_2 axis in the meso diastereoisomers, the two deuterons are enantiotopic, and so magnetically equivalent. The magnitude of $\Delta\nu_Q$ as well as the position of ^{13}C lines are arbitrarily chosen. Due to weakness of the ^{2}H chemical shift anisotropy, all ^{2}H quadrupolar doublets are centered at the same chemical shift. The ^{13}C–{^{1}H} spectral pattern associated to asymmetric carbons (for mixtures **1** and **2**) are in principle identical to that expected for carbon sites 1–6 in mixture **1**. However, generally the ^{13}C chemical shift anisotropy for sp^3 hybridized carbons is much smaller than for aromatic sp^2 hybridized carbons, and hence only small spectral separations for the three isomeric species are expected for these sites.

that diastereoisomeric species and detection sensitivity discriminated by the polypeptide liquid crystals and spectral separation are sufficiently large to prevent tiresome overlaps, as schematically depicted in Fig. 1 [6]. Two of the three originate from the discrimination of enantiotopic deuterons associated with the *meso* isomers (*RS* = *SR*) [7], the two others originating from the discrimination of enantiotopic ones (*RR* and *SS*).

From the ^{13}C–{^{1}H} NMR point of view, the mixtures **1** and **2** must be considered separately. For mixture **1**, four ^{13}C resonances are expected to be observed for each of the equivalent carbon site in the three stereoisomeric species spectrally discriminated on the basis of ^{13}C chemical shift anisotropy differences (CSA) (see Fig. 1) [3]. This occurrence will be also encountered for mixture **2**, except for the ^{13}C sites labelled 3 and 6 for which only three distinct resonances are expected to be detected if all signals are well resolved (see Fig. 1). Indeed, these carbon-13 sites belonging to the symmetry plane in the *meso* molecule, and hence they cannot be differentiated.

From an analytical point of view, the spectral discrimination of stereoisomers based on $\Delta\nu_Q$s is generally more efficient than based on ^{13}C CSA [2,3]. Consequently, the central question arising here is how to analyze and assign quadrupolar doublets belonging to *u*// diastereoisomers, in particular when the enantiomeric and diastereoisomeric excesses are both equal to 0%. Indeed in this particular case, four quadrupolar doublets of identical intensity should be theoretically observed, and so their assignment is not straightforward.

The solution for solving this problem is not unique as we will see below, and various homo- and heteronuclear 2D NMR approaches will be presented in this methodological article, along with their evaluation on test molecules. As seen from the calculated transfer efficiency, the most appropriate strategies will mainly depend on the structure of the molecules under investigation and of their orientation. The actual possibility to generate heteronuclear polarization transfers to separate the useful NMR information heavily system-dependent. The initial goal could not be fully reached on mixtures **1** and **2**, but the steady development of new or improved chiral liquid crystals could help solving this issue.

2. Results and discussion

2.1. Overview of possible 2D NMR strategies

Considering the structure of molecules involved in mixtures **1** and **2**, several possible 2D NMR strategies can be proposed to facilitate the assignment of the quadrupolar doublets for *meso* and enantiomeric compounds, and subsequently to ease their diastereoisomeric excess when known the major diastereoisomer.

The general principle of these ^{2}H assignment strategies is based on the fact that only the *meso* compound possesses two deuterons that can be potentially correlated. Three possibilities can be proposed: (i) the use of ^{2}H–^{2}H correlations through direct dipolar couplings (see Fig. 2a), (ii) the ^{2}H–^{2}H correlations *via* multiple polarization transfers involving heteronuclear atoms (^{1}H or ^{13}C) as relays (see Fig. 2b–f), (iii) the use of ^{2}H–^{13}C correlations if a specific spectral resolution exists, that can be exploited in ^{13}C NMR (see Fig. 2g and h).

The 5th latest approach is based on the correlation of quadrupolar doublets through the existence of ^{2}H–^{2}H total couplings in the various isomers. This strategy using ^{2}H–^{2}H

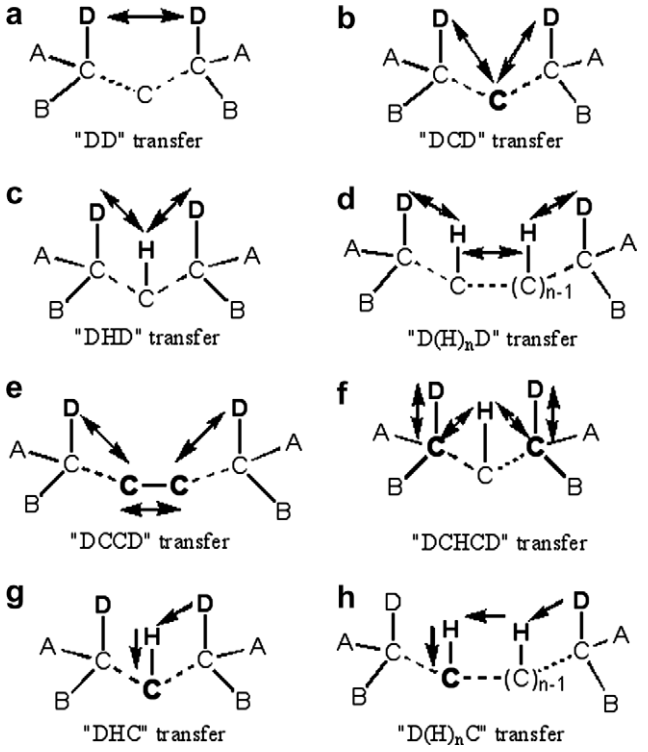

Fig. 2. Examples of (a–f) two- and (g and h) heteronuclear NMR strategies to analyse the structures **1** and **2**, and the following one, two or four heteronuclear (s) assignments.

COSY [2] experiments was successfully applied to analyse and assess diastereoisomeric and dynamic purity in *u/l* mixture where stereoisomers possessed a "Cl_2" group [8,9]. Unfortunately for more remote deuterons (as in the case of mixtures **1** and **2**), the scalar coupling is still weak in the magnitude of ^2H–^2H dipolar coupling is predicted to be too small when weakly oriented liquid crystals, as organic solutions of polypeptides, is used. Chiral molecular orienting esophases could be suggested to increase the solute orientation and so produce larger dipolar couplings. However the existing esophases show generally small orientation bad organic solvents [10]. Other heteronuclear strategies involving either ^2H–^{13}C or ^2H–^1H heteronuclear polarization transfers can be proposed, as shown in Fig. 2. The strategies b, c and d can be proposed to analyze mixture **2** while strategies a and e are adapted to analyze mixture **1**. Note however that strategies e and f are very difficult to apply in the case of non-^{13}C-enriched compounds due to low probability to find isotopomers with two ^{13}C nuclei. Finally, in the case of mixture **2**, heteronuclear strategies g and h, involving one or two proton relays can be valuable to correlate the deuterons to carbon site 6 (eventually site 3) that belongs to the same molecular symmetry.

2.2. The "DCD" correlation experiments

Recently, we have described the HECADE [11] experiments to correlate the ^2H signals of two geminal deuterons to the ^{13}C nucleus [11]. Two methods of polarization transfers using either HSQC- or HMQC-type sequences were explored [12,13]. In Fig. 3a is shown the HECADE-HMQC-4 sequence.

After a four-step phase cycle and dissymmetrization relaxation terms and phase factors, the expression of correlation peaks (CPs) is

$$S_{CP}(t_1,t_2) \propto \tfrac{2}{3}i\times\left\{\sin\left[2\pi\nu_{D_{i,j}}(t_1+\tau)\right]\times\cos\left[\pi\Delta\nu_{Q^{i,j}}(t_1+\tau)\right]\right\}\times f_{corr}(\tau,\tau')\times\left\{\begin{matrix} e^{i\left[2\pi\nu_{D_{j,i}}(\tau+t_2)-\pi\Delta\nu_{Q^{j,i}}(\tau+t_2)\right]} \\ +e^{i\left[2\pi\nu_{D_{j,i}}(\tau+t_2)+\pi\Delta\nu_{Q^{j,i}}(\tau+t_2)\right]}\end{matrix}\right\} \quad (1)$$

where $f_{corr}(\tau,\tau')$ is the transfer function governing the amplitude of correlation peaks of the 2D map [14]. For the "D_{Cl}" pulse sequence, $f_{corr}(\tau,\tau')$ is:

$$f_{corr}(\tau,\tau') = \left\{\begin{matrix}\sin\left[\pi T_{Cl_{i,j}}(\tau)\right]\times\sin\left[2\pi T_{Cl_{i,j}}(\tau')\right] \\ \times\sin\left[2\pi T_{Cl_{j,i}}(\tau')\right]\times\sin\left[\pi T_{Cl_{j,i}}(\tau)\right]\end{matrix}\right\} \quad (2)$$

In these equations, $\nu_{D_{i,j}}$ and $\Delta\nu_{Q^{i,j}}$ are the refocused frequency offsets and quadrupolar splittings of i and j deuterons, respectively, while $T_{Cl_{i,j}}$ is the ^{13}C–^2H total coupling ($T_{Cl_{i,j}} = J_{Cl_{i,j}} + 2D_{Cl_{i,j}}$). Note that Eqs. (1) and (2) were calculated with the help of product-operators for AX systems with $I = 1$ and $S = 1/2$ that was proposed recently [11]. In all heteronuclear ^2H–^2H correlation experiments, diagonal peaks (I_{CP}s) and autocorrelation peaks (A_{CP}s) are also present that the 2D map (for illustration, see Fig. 4a) but only the equations of CPs, that contain the useful information, will be given in this work.

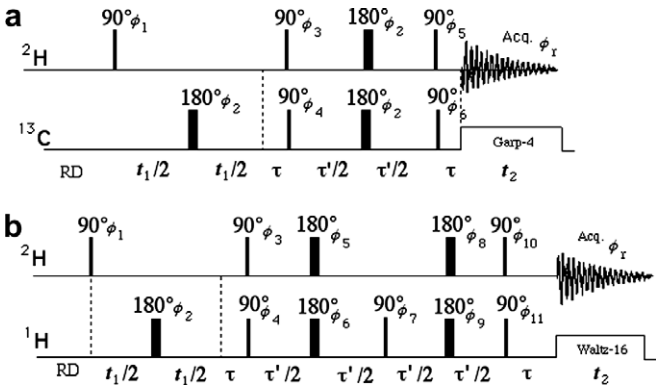

Fig. 3. (a) Pulse sequence of the HECADE-HMQC-4 sequence. The basic four-step phase cycling is: $\phi_1 = 2(x)$, $2(-x)$; $\phi_2 = \phi_3 = \phi_5 = \phi_6 = 4(x)$; $\phi_4 = 2(x,-x)$; $\phi_r = x,-x,-x,x$. GARP-4 sequence suppresses ^{13}C–^2H couplings during the acquisition period. When required, the ^2H nuclei are decoupled by applying the WALTZ-16 pulse sequence over the sequence. (b) Pulse sequence of the "$D_{HH}D_{Cl}$" 2D sequence. The basic four-step phase cycling is: $\phi_1 = 2(x)$, $2(-x)$; ϕ_2, ϕ_3, ϕ_5 to $\phi_{11} = 4(x)$; $\phi_4 = 2(x,-x)$; $\phi_r = x, -x, -x, x$. To correct saturation pulses imperfections, the phase cycling can be extended to eight steps where $\phi_{10} = 4(x)$, $4(-x)$ and $\phi_r = x,-x,-x,x,-x,x,x,-x$, while for other pulses, the four-step phase cycling is repeated twice.

Eq. (2) shows that the intensity of CPs (I_{CP}) varies with delay τ and τ'. In the ideal case, where $|T_{Cl,i}| = |T_{Cl,j}| = |T_{Cl}|$, and disregarding relaxation effects, I_{CP} is maximized with $\tau = 1/2(|T_{Cl}|)$ and $\tau' = 1/(4|T_{Cl}|)$ [11]. Actually, the ideal case where $|T_{Cl,1}| = |T_{Cl,2}|$ (for a "^{1}H–^{13}C–^{2}H" system) does not exist, but generally a good compromise is obtained by averaging the T_{Cl} values.

This sequence was successfully tested in the case of gem-dideuterated solids to analyse the anisotropic ^2H_i–{^1H_i} spectra of a mixture of two deuterated pharmaceutical compounds [11]. Assuming that the $^3T_{Cl}$ coupling is not known, such an approach seems well-adapted for analyzing mixture **2**, because where the carbon atom labelled 6 (see Fig. 1) could play the same role as the ^{13}C atom in the CH_2 group. Unfortunately, no three-bond C–H total coupling was observed in the various deuterated isomers of mixtures **2**, mainly due to the long distance between ^{13}C and ^{2}H sites and the weak alignment of solutes in polypeptide mesophases.

Fig. 4. Experimental 92.1 MHz "^1H_i–^1H_j" 2D spectra of **3** (a) and **4** (b) dissolved in PBLG/$CHCl_3$ phase at 300 K. The 2D matrix is 256 (t_1) × 1538 (t_2) data points, with NS = 32 (a) and 512 (t_1) × 2048 (t_2) data points, with NS = 8 (b). Exponential filtering (1 Hz) in F_2 and F_1 dimensions is applied in both experiments. On the 2D map (a), the diagonal peaks (DP), autocorrelation peaks (AP) and cross-correlation peaks (CP) associated with the H_2 and H_4 deuterons are labelled.

2.3. The "DHD" correlation experiments

An alternative to the "^1H_i–$^{13}C_i$" experiment consists in using experiments with a "^1H_i–^2H_j"-type transfer where the carbon relay is replaced by a proton relay. In this new sequence, the ^2H magnetization is transferred *via* the highly abundant proton nucleus (99.985%) thus increasing the intrinsic sensitivity of the experiment. In addition, we benefit from a nucleus with an agetogyric ratio four times less than the one of carbon. Hence, in the particular case of mixture **2**, we can *a priori* expect larger dipolar couplings between deuterons and $^1H^6$ than between deuterons and C^6.

The "^1H_i–^2H_j" pulse sequence is identical to the 1D ECA-LEMCYCLOPES sequence but the proton nucleus plays the role of the ^{13}C nucleus. Nevertheless, from the polarization transfer point of view, the situation can be more complex than for "^1H_i–$^{13}C_i$" transfers as proton(s) relaying the single quantum coherences (SQC's) can be also coupled with other surrounding protons in the molecule. This occurrence does not exist for the "^1H_i–$^{13}C_i$" transfers due to the low abundance of isotopomers with two ^{13}C nuclei.

After a four-step phase cycle and disregarding all relaxation terms, the expression of CPs for the "^1H_i–^2H_j" sequence is formally identical to Eq. (1), but the transfer function can differ according to the ^1H–^1H coupling pattern. For a simple system "^1H_i–^2H_j($^1H^1$)–$^1H^j$" where the $^1H_{i,j}$ are coupled to an equivalent proton, $^1H^1$, weakly coupled themselves to several protons, $^1H^j$ (equivalent or not), f_{corr} is equal to:

$$f_{corr}(\tau,\tau') = \tfrac{1}{2} \times \left\{ \begin{array}{l} \sin[\pi T_{1_i,1^1}\tau]\cos^{n-1}[\pi T_{1_i,1^1}\tau] \\ \times \sin[2\pi T_{1_i,1^1}\tau']\sin[2\pi T_{1_i,1^1}\tau'] \\ \times \cos^{n-1}[3\pi D_{1_i,1^1}\tau']\left\{\prod_j \cos[\pi T_{1^1,1^j}\tau']\right\} \\ \times \sin[\pi T_{1_j,1^1}\tau]\cos^{n-1}[\pi T_{1_j,1^1}\tau] \end{array} \right\} \quad (3)$$

The choice of the τ delay for maximizing f_{corr} depends both on the $T_{1^1,1^j}$ values and the number (n) of protons which contribute to the relay. In the ideal case where $|T_{1_i,1^1}| = |T_{1_j,1^1}| = |T_{1^1,1^j}|$, the maximum transfer during τ delay occurs with $\tau = 1/|2T_{1^1,1^j}|$, $1/|4T_{1^1,1^j}|$ and $0.196/|T_{1^1,1^j}|$ for a pair, a triplet, a quartet (n protons are equivalent), and a methyl group, respectively [15]. The choice of τ' is less trivial due to its dependency on the magnitude of (i) ^2H_i–^1H_i total couplings, (ii) ^1H_i–^1H_j total couplings if the proton(s) participating to the relay is (are) also coupled with other equivalent protons, (iii) the ^1H_i–^1H_j dipolar coupling between the equivalent protons involved in the relay. In the simple, ideal case where $|T_{1_i,1^1}| = |T_{1_j,1^1}| = |T_{1^1,1^j}|$ and $|D_{1_i,1^1}| = |T_{1_i,1^1}| = 0$, then we have $\tau' = 1/|4T_{1^1,1^j}|$. As for the "^1H_i–$^{13}C_i$" experiments, the average of $|T_{1^1,1^j}|$ provides a suitable value for experimentally optimizing the polarization transfers.

Although the relaxation terms were not shown in Eq. (3), the efficiency of f_{corr} is not independent of T_2 relaxation effect [14]. Thus in the general case, we can show that

$f_{corr}(\tau,\tau')$ depends on the exponential term $\exp(-\tau/T_2^{i})\exp(-\tau'/T_2^{n})\exp(-\tau/T_2^{j})$. *A priori*, the choice of τ and τ' depends on the T_2 times of deuterons and protons, respectively. In practice, as $T_2^{H} \approx |1/T_{1H}|$, the τ delays must be systematically compared to the ideal value in order to minimize the losses due to the T_2 relaxation. In contrast, as generally $T_2^{H} \geqslant |1/T_{1H}|$, the optimal τ' value can be chosen independently of the T_2^{H} value.

To experimentally test this sequence, we chose two model molecules, the 2,4,6-trideuterated-3-ethyl phenol (**3**) and 2,4,6-trideuterated-1-ethanol (**4**) dissolved in mesophases made of poly-γ-benzyl-L-glutamate (PBLG) and $GeCl_3$ or poly-ε-carbobenzyloxy-L-lysine (PCBLL) and $GeCl_3$ (see Table 1). These aligned solutes (see Fig. 4) are ideal testing theoretical and experimental models for various reasons. First, the couplings between deuterons are small or too small and cannot generate direct correlations that could be erroneously interpreted as correlations due to the "I_2H_1" transfers. Second, the heteronuclear $^2H_1$–$^1H_1$ total couplings over four bonds are null in **3** and **4**, thus limiting the number of terms in f_{corr}. Third, these solutes allow testing the "I_2H_1" transfers *via* different protons in the systems. To visualize in Fig. 3, the "I_2H_1" transfers can be investigated either a single proton, H_1^5 (coupled or not to ethyl group protons, H_1^7) or the three equivalent protons of ethyl group (coupled or not to proton H_1^5). For **4**, we can consider a "I_2H_1" transfer using a single proton, that can be a priori involved either in the A_2 or AA′ spin system. These differences in proton spin systems affect the expression of the transfer function, $f_{corr}(\tau,\tau')$.

For **3**, and assuming that $^5T_{H_1H_1^7}$ is null, the transfer function between I_1^4 and I_1^6 is similar to Eq. (3), except that carbon subscripts are replaced by the proton subscripts. In contrast, H_1^5 and H_1^7 are weakly coupled, we have to reason in the AX_3 proton spin system, and a new term depending on the $^5T_{H_1H_1^7}$ coupling appears in $f_{corr}(\tau,\tau')$:

$$f_{corr}(\tau,\tau') = \left\{ \begin{array}{l} \sin\left[\pi^3 T_{1_{4,6}H_1^5}\tau\right] \\ \times \sin\left[2\pi^3 T_{1_{4,6}H_1^5}\tau'\right] \sin\left[2\pi^3 T_{1_{4,6}H_1^5}\tau'\right] \\ \times \cos^3\left[\pi^5 T_{H_1^5H_1^7}\tau'\right] \\ \times \sin\left[\pi^3 T_{1_{4,6}H_1^5}\tau\right] \end{array} \right\} \quad (4)$$

Experimentally, the evolutions of I_1^4 and H_1^5 are not coupled to each other, thus giving the possibility to correlate I_1^4 to I_1^6 through H_1^5.

In compound **3**, a second type of transfer is possible through the three equivalent protons of ethyl group, H_1^7. Assuming that the total coupling $^5T_{H_1^5H_1^7}$ is not null, the transfer function between I_1^2 and I_1^4 is now governed by the following equation:

$$f_{corr}(\tau,\tau') = 9 \times \left\{ \begin{array}{l} \sin\left[\pi^4 T_{1_{2,4}H_1^7}\tau\right]\cos^2\left[\pi^4 T_{1_{2,4}H_1^7}\tau'\right] \\ \times \sin\left[2\pi^4 T_{1_{2,4}H_1^7}\tau'\right]\sin\left[2\pi^4 T_{1_{4,3}H_1^7}\tau'\right] \\ \times \cos^2\left[3\pi^2 D_{H_1^7H_1^7}\tau'\right]\cos\left[\pi^5 T_{H_1^5H_1^7}\tau'\right] \\ \times \sin\left[\pi^4 T_{1_{4,3}H_1^7}\tau\right]\cos^2\left[\pi^4 T_{1_{4,3}H_1^7}\tau\right] \end{array} \right\} \quad (5)$$

Note that the $\cos[\pi^5 T_{H_1^5H_1^7}\tau']$ term becomes equal to 1 when $^5T_{H_1^5H_1^7} = 0$.

Fig. 4a shows the "I_2H_1" 2D map of **3** when the polarization transfers involves protons of the ethyl group. We have experimentally observed the existence of proton–proton couplings between ethyl protons and H_1^5, and the sequence $f_{corr}(\tau,\tau')$ is given by Eq. (5). The ideal values for τ should correspond to $0.196/|^4T_{1H}|$, assuming that the $|^4T_{1_{3H_1^7}}| = |^4T_{1_{4H_1^7}}| = |^4T_{1H}|$. In practice, the optimal value of τ is found to be equal to 19.8 ms, thus corresponding to a good balance between the defocusing due to the T_{2H} couplings (≈8.5 Hz) and the T_2 relaxation times for I_1^6 and I_1^4(≈57 ms). On the other hand, the τ' optimal value ($\tau' = 35.4$ ms) is determined by taking into account the H_1^5–H_1^7 total coupling (7 Hz) and the H_1^7–H_1^7 dipolar coupling (8 Hz). As expected on the 2D map, CHs arise only between I_1^2 and I_1^4 (see Fig. 4a) while the I_1Hs and A_1Hs are observed for all deuterons, including also I_1^6 due to the coupling between I_1^6 and H_1^5. The difference of intensity in I_1Hs and A_1Hs for I_1^2 and I_1^4 results from the choice of both τ and τ' values [11].

As compound **4** has a C_{2v} symmetry, the H_1^3 and H_1^5 protons belonging either to an AA′ or to an A_2 spin system designated H_1^3 and H_1^5 are coupled or not. Due to the second order nature of an AA′ spin system, the analytical expression of $f_{corr}(\tau,\tau')$ is very complex to calculate, and was not established. Experimentally, the analysis of both ^1H–{^1H} and ^2H–{^1H} spectra indicates that the proton

Table 1
Labelling and composition of the liquid–crystalline samples used in the present work

Solute	Solute (mg)	PBLG[a] (mg)	PCBLL[b] (mg)	$GeCl_3$ (mg)	% of polymers (wt)
1	17	130	0	413	23.2
2	21	0	100	451	17.5
3	11	101	0	404	19.5
3	12	0	99	470	17.0
4	10	100	0	424	18.8
5[c]	75	101	0	454	15.9

[a] The M_w of PBLG is 782.
[b] The M_w of PCBLL is 778.
[c] The ee is over 95%.

is an A_2 spin system with no H–H dipolar coupling. Hence, in this case, $f_{corr}(\tau,\tau')$ is equal to:

$$f_{corr}(\tau,\tau') = 2 \times \left\{ \begin{array}{l} \sin[\pi^3 T_{D4H3,5}\tau]\cos[\pi^3 T_{D4H3,5}\tau] \\ \times\sin[2\pi^3 T_{D4H3,5}\tau']\sin[2\pi^3 T_{D2,6H3,5}\tau'] \\ \times\sin[\pi^3 T_{D2,6H3,5}\tau] \end{array} \right\} \quad (6)$$

Fig. 4b shows the "DHD" 2D map of 4 where the correlations between D^2(D^6) and D^4 were successfully observed. In this second example, the optimal values of τ and τ' were found to be equal to 15.2 and 17.4 ms. As previously, the difference of intensity in DPs and APs results from the choice of τ and τ' values.

2.4. The "DHHD" correlation experiments

The "DHHD" 2D sequence is a variation of the "DHD" 2D pulse sequence in which a 90° pulse is introduced in the middle of the τ' period in order to relay the ^1H magnetization between neighbor protons. The sequence is depicted in Fig. 3b. During the τ' delays, the H SQCs evolve under the effect of couplings $|T_{DH}|$ and $|T_{HH}|$. Thus during the two first $\tau'/2$ delays, the ^1H magnetization, antiphase with respect to H–^{2}H coupling, is converted into H magnetization, antiphase with respect to H–H coupling. During the two last $\tau'/2$ delays, the previous mechanism is reversed. The two pairs of simultaneous H and ^{2}H 180° pulses implemented in the sequence remove the H chemical shifts without affecting the homo- and heteronuclear couplings.

After a four-step phase cycle, the analytical expression of CP signals is formally identical to Eq. (1) but $f_{corr}(\tau,\tau')$ differs from that obtained in the "DHD" transfer. Thus, in the case of a spin system of the form "D^i–H^k–H^l–D^j" where H^k and H^l are weakly coupled, $f_{corr}(\tau,\tau')$ is equal to:

$$f_{corr}(\tau,\tau') = (n \times m)^2 \times \left\{ \begin{array}{l} \sin[\pi T_{D^iH^k}\tau]\cos^{n-1}[\pi T_{D^iH^k}\tau] \\ \times\sin[2\pi T_{D^iH^k}\tau']\cos^{n-1}[3\pi D_{H^kH^k}\tau'] \\ \times\sin[\pi T_{H^kH^l}\tau']\cos^{m-1}[\pi T_{H^kH^l}\tau'] \\ \times\sin[2\pi T_{D^jH^l}\tau']\cos^{m-1}[3\pi D_{H^lH^l}\tau'] \\ \times\sin[\pi T_{H^kH^l}\tau']\cos^{n-1}[\pi T_{H^kH^l}\tau'] \\ \times\sin[\pi T_{D^jH^l}\tau]\cos^{m-1}[\pi T_{D^jH^l}\tau] \end{array} \right\} \quad (7)$$

In Eq. (7), the relaxation terms have been disregarded, but in the general case, we can show that $f_{corr}(\tau,\tau')$ is weighted by a $\exp(-\tau/T_2^{D^i})\exp(-\tau'/T_2^{H^k})\exp(-\tau'/T_2^{H^l})\exp(-\tau/T_2^{D^j})$ factor. Here again, the optimal τ delay is dependent on the T_2^D values, and thus will be generally shortened compared to the ideal value to minimize losses due to T_2 relaxation.

For illustration, compound 3 can be used as an interesting example since the coupling between H^7 and H^5 is not null (see above). Under this condition, it is possible to generate a correlation between deuterons D^2 and D^6 through H^7 and H^5. However in this case, an additional term of the form, $[1+2\cos(2\pi^4 T_{D4H7}\tau')]/3$ must be included in f_{corr}, since the H SQCs of the methyl group also evolve under the effect of the coupling with D^4 (see above).

Using deuterium and proton notations associated with compound 3, $f_{corr}(\tau,\tau')$ becomes:

$$f_{corr}(\tau,\tau') = 9 \times \left\{ \begin{array}{l} \sin[\pi^4 T_{D2H7}\tau]\cos^2[\pi^4 T_{D2H7}\tau] \\ \times\sin[2\pi^4 T_{D2H7}\tau'][1+2\cos(2\pi^4 T_{D4H7})\tau']/3 \\ \times\sin[\pi^5 T_{H5H7}\tau']\cos^2[3\pi^2 D_{H7H7}\tau'] \\ \times\sin[2\pi^3 T_{D6H5}\tau']\sin[\pi^5 T_{H5H7}\tau']\cos^2[\pi^5 T_{H5H7}\tau'] \\ \times\sin[\pi^3 T_{D6H5}\tau] \end{array} \right\} \quad (8)$$

Fig. 5 shows the "DHHD" 2D map of 3 where the homonuclear correlations between D^2 and D^6 were successfully observed. In this second example, the optimal τ value is equal to 18.5 ms, and results from a compromise between the theoretical ideal value and the short T_2 values for deuterons (≈57 ms). From Eq. (8), the optimal τ' value is 81.8 ms.

Similarly to the "DHD" 2D map shown in Fig. 4a, we might expect to see the DPs and APs associated with the passive deuteron, D^4, as well as CPs between D^4 and D^6, but the choice of τ and τ' values leads to no visible peaks (even at very low level). Finally it could be noted that the central 90° pulse used for relaying proton magnetization can be replaced by a MLEV-type sequence framed with two trim pulses that should be a reliable method to transfer H polarization through more than two protons [16,17].

2.5. The "DHC" and "DHHC" correlation experiments

The "DHC" or "DHHC" correlation 2D experiments can be very efficient to analyse the case of mixture 2. Indeed, as described above, the carbon atoms, noted 6 and 3, for *meso* compound in mixture 2 belong to the plane of symmetry, and so cannot show two separate resonances contrarily to the 1/5 and 2/4 carbon atom pairs. Conse-

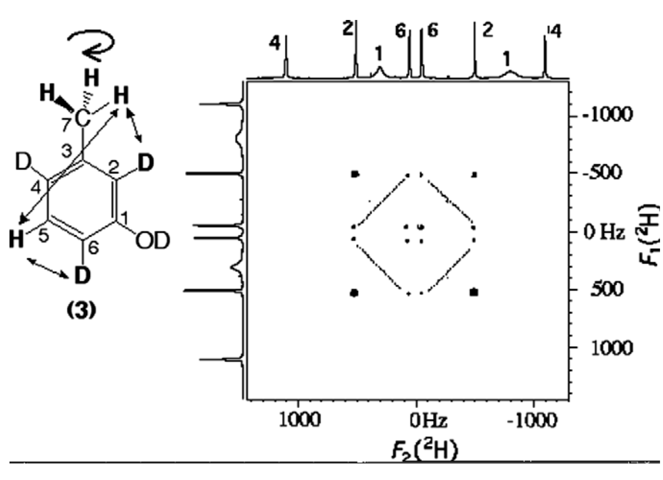

Fig. 5. Experimental 92.1 MHz "DHHD" 2D spectra of 3 in PBLG/$CHCl_3$ phase at 300 K. The 2D matrix is 256 (t_1) × 1538 (t_2) data points, with NS = 288. Exponential filtering (3 Hz) in F_2 and F_1 dimensions is used. The 2D map is symmetrised.

sequently, taking advantage of this particular spectral feature associated with the molecules of mixture **2**, we should be able to assign the diastereoisomeric ^2H doublets from $^2H/^{13}C$ correlations.

The "DHC" pulse 2D sequence proposed here is shown in Fig. 6a and b. For such an experiment, the DPs and APs do not exist, thus strongly reducing the number of peak in the 2D map.

Whereas the beginning of the sequence is similar to the "DHD" 2D experiment, the second heteronuclear INEPT transfer converts the ^1H SQCs into an observable ^{13}C magnetization during acquisition. The combination of three 180° pulses implemented as shown in Fig. 6 (top and middle) allows the evolution of ^2H SQCs under the effect of ^2H–^1H and ^1H–^{13}C couplings with elimination of the ^2H chemical shift evolution when $\tau_1 = \tau_2 + \tau_3$ [18]. In practice, the position of ^2H and ^{13}C 180° pulses depends on the magnitude of $|2T_{DH}|$ and $|T_{CH}|$. Fig. 6a and b present the "DHC" sequence that must be used when $|2T_{DH}| < |T_{CH}|$ and $|2T_{DH}| > |T_{CH}|$, respectively. As seen, the triggering order of ^{13}C and ^1H 180° pulses in both sequences is simply reversed. Finally, if the proton (or group of equivalent protons) used as relay is also coupled with other protons, then the ^1H magnetization evolves also under the effect of coupling, $|T_{HH}|$ during $\tau_1 + \tau_2 + \tau_3$.

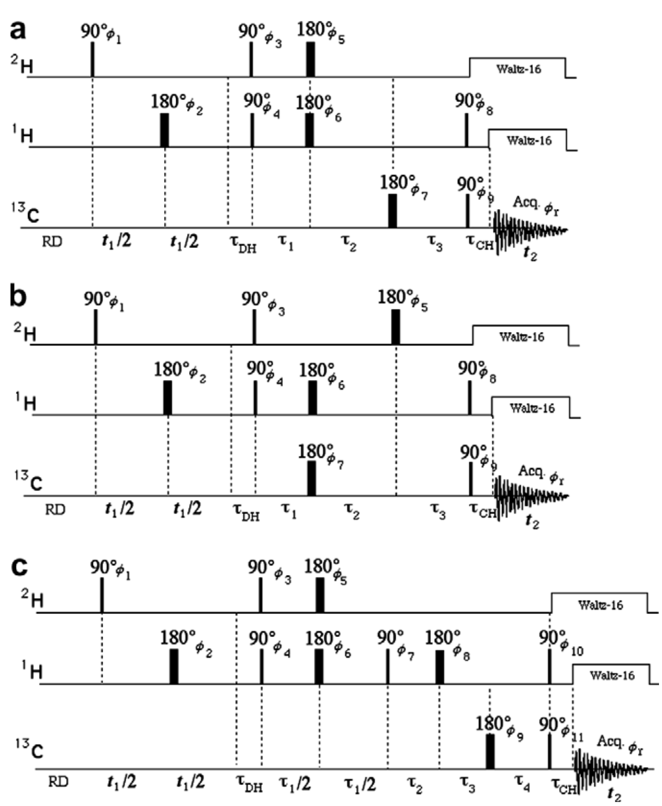

Fig. 6. Pulse schemes of the (a and b) "DHC" and (c) "DHHC" sequences using two INEPT-type transfers. Sequence a (b) is applied when $|2T_{DH}| < |T_{CH}|$ ($|2T_{DH}| > |T_{CH}|$). The basic two-step phase cycling is: (a and b) $\phi_1 = x, -x$; ϕ_2 to $\phi_9 = x, x$; $\phi_r = x, -x$; and (c) $\phi_1 = x, -x$; ϕ_2 to $\phi_{11} = x, x$; $\phi_r = x, -x$.

After a two-step phase cycle and disregarding the relaxation term, the general form of expression of the NMR signal for an "DHC" 2D experiment is given by:

$$S(t_1,t_2) \propto \left\{ \begin{array}{l} \cos[(2\pi\nu_D + \pi\Delta\nu_Q)(t_1+\tau_{DH})] \\ + \cos[(2\pi\nu_D - \pi\Delta\nu_Q)(t_1+\tau_{DH})] \end{array} \right\} \times f_{corr}(\tau_{DH},\tau_1,\tau_2,\tau_3,\tau_{CH}) \times \{e^{i[2\pi\nu_C(\tau_{CH}+t_2)]}\} \quad (9)$$

As previously, $f_{corr}(\tau_{DH},\tau_1,\tau_2,\tau_3,\tau_{CH})$ is the transfer function. For simplifying notations, we will denote hereafter $f_{corr}(\tau_{DH}, \tau_1, \tau_2, \tau_3, \tau_{CH})$ as $f_{corr}(\tau_n)$. For a "D^i–$H^k_n(H^l)$–C^j" spin system where H^k and H^l protons are weakly coupled, its analytical expression is:

$$f_{corr}(\tau_n) = n^2 \times \left\{ \begin{array}{l} \sin[\pi T_{D^iH^k}\tau_{DH}]\cos^{n-1}[\pi T_{D^iH^k}\tau_{DH}] \\ \times \sin[2\pi T_{D^iH^k}(\tau_1 \pm \tau_2 + \tau_3)] \\ \times \sin[\pi T_{CH^k}(\tau_1 \mp \tau_2 + \tau_3)] \\ \times \cos^{n-1}[3\pi D_{H^kH^k}(\tau_1+\tau_2+\tau_3)] \\ \times \prod \cos[\pi T_{H^kH^l}(\tau_1+\tau_2+\tau_3)] \\ \times \sin[\pi T_{CH^k}\tau_{CH^k}]\cos^{n-1}[\pi T_{CH^k}\tau_{CH^k}] \end{array} \right\} \quad (10)$$

with setting $\tau_1 = \tau_2 + \tau_3$. As seen in Eq. (10) (lines 2 and 3), the effective evolution periods due to couplings T_{DH} and T_{CH} are equal to $(\tau_1+\tau_2+\tau_3)$ and $(\tau_1-\tau_2+\tau_3)$, for the first sequence, and $(\tau_1-\tau_2+\tau_3)$ and $(\tau_1+\tau_2+\tau_3)$ for the second one.

Assuming no ^1H–^1H couplings, then $f_{corr}(\tau_n)$ of the first "DHC" sequence is ideally maximized when $\tau_{DH} = 1/|2T_{DH}|$, $\tau_1 = 1/|8T_{DH}|$, $\tau_2 = 1/|8T_{DH}| - 1/|4T_{CH}|$ if $|2T_{DH}| < |T_{CH}|$, $\tau_3 = 1/4T_{CH}$ and $\tau_{CH} = 1/|2T_{CH}|$. For the second "DHC" sequence, $\tau_1 = 1/|4T_{CH}|$, $\tau_2 = 1/|4T_{CH}| - 1/|8T_{DH}|$ and $\tau_3 = 1/|8T_{DH}|$. From a relaxation point of view, $f_{corr}(\tau_n)$ depends on the following term $\exp(-\tau_{DH}/T_2^{D^i})\exp(-(\tau_1+\tau_2+\tau_3)/T_2^{H^k})\exp(-\tau_{CH}/T_2^{C^j})$ in both sequences. Comparing the $1/T_{ij}$ values to the ^1H, ^2H and ^{13}C T_2 relaxation values, it is clear that only the choice of τ_{DH} can be affected by the T_2 relaxation.

To illustrate the efficiency of the "DHC" sequence in oriented media, we have analysed the case of compounds **5** and **3**. For **5**, the "DHC" transfer involves a single proton as relay while for **3**, the transfer implicates three equivalent protons that are dipolar coupled. For solute **5**, the condition $|2T_{DH}|$ (=10 Hz) < $|T_{CH}|$ (=208 Hz) is experimentally fulfilled, and so the first "DHC" pulse sequence (Fig. 6a) must be applied. Assuming that D^1 is only coupled with proton H^8, itself weakly coupled to H^7, the expression of $f_{corr}(\tau_n)$ is:

$$f_{corr}(\tau_n) = \left\{ \begin{array}{l} \sin[\pi^4 T_{D^1H^8}\tau_{DH}] \\ \times \sin[2\pi^4 T_{D^1H^8}(\tau_1+\tau_2+\tau_3)] \\ \times \sin[\pi^1 T_{C^8H^8}(\tau_1-\tau_2+\tau_3)] \\ \times \cos[\pi^3 T_{H^7H^8}(\tau_1+\tau_2+\tau_3)] \\ \times \sin[\pi^1 T_{C^8H^8}\tau_{CH}] \end{array} \right\} \quad (11)$$

Fig. 7a presents the "$^1H,^{13}C$" 2D map obtained for **5** with the refocusing delays of the "$^1H,^{13}C$" sequence optimized for correlating deuterium ^{1} to carbon C^8. No fourth correlation is observed on the 2D map, probably since the coupling between ^{1} and the axial and equatorial protons, H^2, of cyclohexyl ring are null. To this example, it is interesting to emphasize that the assignment of the ^{13}C peak at around 128.5 ppm is not trivial using, the additivity rules of substituents for instance, and contradictory assignments for carbon atoms, C^5 and C^8, can be found using NMR data bases or prediction softwares such as ACD. The results obtained here allow to assign unambiguously the carbon signal C^8 on the aromatic group. This assignment has been confirmed by recording the NMR EQUATE 2D experiment of **5** in isotropic phase [19].

For compound **3** dissolved in the PCB/G/CDCl$_3$ (see Table 1), we find $|2T_{HH}|$ (=60 Hz) > $|T_{CH}|$ (=32 Hz), and hence the second "$^1H,^{13}C$" pulse sequence must be applied. If the expression of the NMR signals of the 2D map is

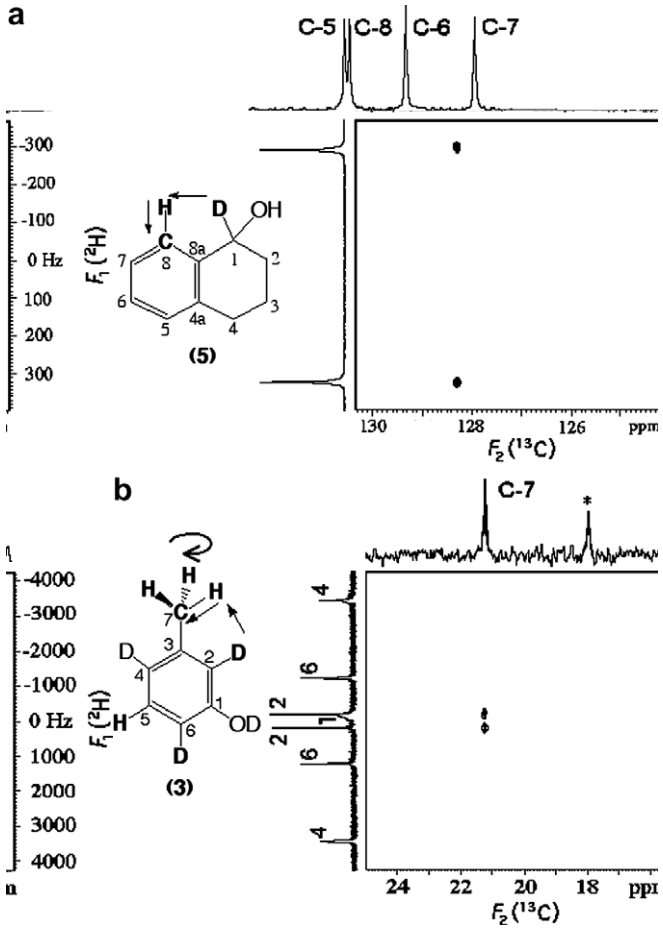

Fig. 7. Experimental 100.6 MHz "$^1H,^{13}C$" 2D spectra of **5** (a) and **3** (b) recorded in PBLG/CHCl$_3$ and PCB/G/CHCl$_3$ at 300 K. The 2D matrix is 128 (t_1) × 2048 (t_2) data points, with NS = 1024 for (a) and (b). The delays τ_{HH}, τ_1, τ_2, τ_3 and τ_{CH}, are equal to 56.5, 14.0, 12.8, 1.2 and 2.4 ms for (a) and 2.5, 8.2, 6.4, 1.8 and 6.2 ms for (b). The peak labeled with an asterisk corresponds to the ^{13}C signal of the ethyl group of ethanol used for stabilizing the orientation.

identical to Eq. (9), the transfer function is multiplied by the evolution under the effect of the heteronuclear coupling between I^4 and H^7 undergoing the effective period $\tau_1 - \tau_2 + \tau_3$. Thus we have:

$$f_{corr}(\tau_n) = 9 \times \left\{ \begin{array}{l} \sin[\pi^4 T_{I^4H^7}\tau_{HH}]\cos^2[\pi^4 T_{I^4H^7}\tau_{HH}] \\ \times \sin[2\pi^4 T_{I^4H^7}(\tau_1 - \tau_2 + \tau_3)] \\ \times (1 + 2\cos[2\pi^4 T_{I^4H^7}(\tau_1 - \tau_2 + \tau_3)])/3 \\ \times \cos^2[3\pi^2 D_{H^2H^7}(\tau_1 + \tau_2 + \tau_3)] \\ \times \cos[\pi^5 T_{H^5H^7}(\tau_1 + \tau_2 + \tau_3)] \\ \times \sin[\pi^1 T_{C^8H^7}(\tau_1 + \tau_2 + \tau_3)] \\ \times \sin[\pi^1 T_{C^8H^7}\tau_{CH}]\cos^2[\pi^1 T_{C^8H^7}\tau_{CH}] \end{array} \right\} \quad (12)$$

The "$^1H,^{13}C$" 2D map obtained for **3** with the defocusing and refocusing delays of "$^1H,^{13}C$" sequence optimized for correlating deuterium ^{2} to carbon C^7 is shown in Fig. 7b. Experimentally, two other correlations was observed. Note here the change of phase of the spin state multiplies the solute orientation, and leads to invert the quadrupolar doublets associated with deuterium ^{2} and ^{6} compared with spectra shown in Figs. 4a and 5.

A possible extension of the "$^1H,^{13}C$" experiment consists of inserting a 90° pulse at the end of the refocusing delay of ^1H–^3H coupling (see Fig. 6c). Thus it becomes possible to transfer ^1H magnetization to another carbon atom through a pair of coupled protons. As in the case of the "$^1H,^{13}C$" sequence, the ideal values for τ_{HH} and τ_{CH} are equal to $1/|2T_{HH}|$ and $1/|2T_{CH}|$. Using the τ_1 delay, the ^1H SQCs evolve under the effect of couplings, T_{HH} and T_{HH}, but the evolution of these coherences under the effect of couplings, T_{CH} and T_{HH}, proceeds for the effective periods $\tau_2 - \tau_3 + \tau_4$ and $\tau_2 + \tau_3 + \tau_4$, respectively.

The expression of the NMR signals for the "$^1H,^1H,^{13}C$" correlation experiment is identical to Eq. (9). However the transfer function differs from that associated with the "$^1H,^{13}C$" experiment. For a "I_i–H_j–H_k–C" spin system, where H_j and H_k equivalent protons are weakly coupled, the analytical expression of $f_{corr}(\tau_{HH}, \tau_1, \tau_2, \tau_3, \tau_4, \tau_{CH})$ (noted here as $f_{corr}(\tau_n)$) is:

$$f_{corr}(\tau_n) = (\quad \times \quad)^2 \left\{ \begin{array}{l} \sin[\pi T_{H_jH_k}\tau_{HH}]\cos^{-1}[\pi T_{H_jH_k}\tau_{HH}] \\ \times \sin[2\pi T_{H_jH_k}\tau_1]\cos^{-1}[3\pi D_{H_jH_k}\tau_1] \\ \times \sin[\pi^1 T_{H_jH_k}\tau_1]\cos^{-1}[\pi T_{H_jH_k}\tau_1] \\ \times \sin[\pi T_{C^iH_j}(\tau_2 - \tau_3 + \tau_4)] \\ \times \cos^{-1}[3\pi D_{H_jH_k}(\tau_2 + \tau_3 + \tau_4)] \\ \times \sin[\pi T_{H_jH_k}(\tau_2 + \tau_3 + \tau_4)] \\ \times \cos^{-1}[\pi T_{H_jH_k}(\tau_2 + \tau_3 + \tau_4)] \\ \times \sin[\pi T_{C^iH_j}\tau_{CH}]\cos^{-1}[\pi T_{C^iH_j}\tau_{CH}] \end{array} \right\} \quad (13)$$

assuming at $\tau_2 = \tau_3 + \tau_4$ in order to eliminate the evolution under ^1H chemical shifts. In the simple case where $m = n = 1$, then the ideal values for the refocusing periods, τ_2, τ_3 and τ_4 are: $\tau_2 = 1/|4T_{HH}|$, $\tau_3 = 1/|4T_{HH}| - 1/|4T_{CH}|$ if

$T_{HH} < T_{CH}$ and $\tau_4 = 1/|4T_{CH}|$. The ideal value for delay τ_1 results in a subtle compromise between the defocusing of ^{1}H magnetization with the T_{DH} coupling and its refocusing with T_{HH} coupling. Mathematically, this value corresponds to the maximum of the function constituted by the four terms depending on τ_1 in Eq. (13).

From a relaxation point of view, we can show that $f_{corr}(\tau_p)$ depends on the following terms:

$$\exp\left(-\tau_{DH}/T_2^{D^i}\right)\exp\left(-\tau_1/T_2^{H^i}\right)$$
$$\exp\left(-(\tau_2+\tau_3+\tau_4)/T_2^{H^j}\right)\exp\left(-\tau_{CH}/T_2^{C^j}\right) \quad (14)$$

As previously, the T_2 relaxation will mainly affect the optimal value of τ_{DH}.

This kind of transfer has been tested on compound **5** where the H^7–H^8 *ortho* coupling is not null (≈33 Hz). Assuming that H^7 is also coupled with H^6, the transfer function, $f_{corr}(\tau_p)$, is equal to:

$$f_{corr}(\tau_p) = \left\{ \begin{array}{l} \sin[\pi^4 T_{D^1H^8}\tau_{DH}] \\ \times \sin[2\pi^4 T_{D^1H^8}\tau_1]\sin[\pi^3 T_{H^7H^8}\tau_1] \\ \times \sin[\pi^3 T_{H^7H^8}(\tau_2+\tau_3+\tau_4)] \\ \times \sin[\pi^1 T_{C^7H^7}(\tau_2-\tau_3+\tau_4)] \\ \times \cos[\pi^3 T_{H^6H^7}(\tau_2+\tau_3+\tau_4)] \\ \times \sin[\pi^1 T_{C^7H^7}\tau_{CH}] \end{array} \right\} \quad (15)$$

Fig. 8 shows the "D–H–H–C" 2D correlation experiment obtained for **5** in the PBLG mesophase. As expected, only the correlation between D^1 and C^7 is observed on the map, thus allowing an easy assignment of ^{13}C signal for carbon 7. The result has been also confirmed using the analysis of the INADEQUATE experiment.

As in the case of "D–(H)$_n$–D" 2D experiment with $n > 2$, the 90° pulse used for ^{1}H relay could be replaced by a MLEV-17 sequence framed with two trim pulses for performing a multiple proton relay.

2.6. Applications to a mixture of deuterated unlike/like stereoisomers

The initial goal of this work was to experimentally separate and assign the ^{2}H signals of *meso* compound and enantiomers in mixtures **1** and **2** oriented in a polypeptide mesophase. Experimentally, we have tested various oriented solvents made of PBLG or PCBLL dissolved in organic solvents such as $CHCl_3$ or DMF. For almost all of those mixtures, we have obtained four separated quadrupolar doublets. The NMR sample composition providing the best spectral discriminations for mixtures **1** and **2** is listed in Table 1. Unfortunately, even varying the composition (in wt%) or/and temperature of the sample, we were not able to detect ^{2}H–^{1}H couplings for the *meso* isomer and enantiomers either in mixture **1** or mixture **2**. The main reasons for these unsuccessful results are both the long distance between D–H in these molecules and the fast rotation of the lateral groups around the sp^2–sp^3 single bonds.

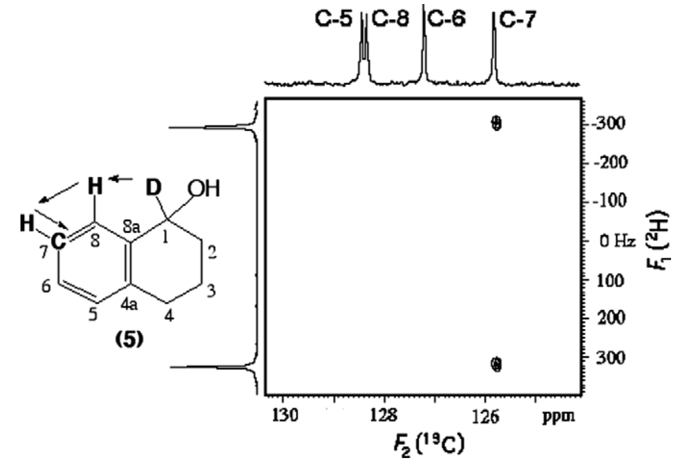

Fig. 8. Experimental 100.6 MHz "D–H–H–C" 2D spectra of **5** in PBLG/$CHCl_3$ phase at 300 K. The 2D matrix is $100(t_1) \times 2048(t_2)$ data points with NS = 1024. The delays τ_{DH}, τ_1, τ_2, τ_3, τ_4 and τ_{CH}, are equal 56.5, 17.0, 3.5, 0, 3.5 and 7.0 ms, respectively.

These unsuccessful experimental results are rather frustrating even though numerical simulations using NMRSIM 4.3 software have shown the ability of "D–H–D" sequences to perform the assignment of a mixture of *u/l* stereoisomers.

To provide an illustrative example of the "D–H–C" 2D spectrum that could be experimentally obtained under ideal conditions, Fig. 9 presents the simulated "D–H–C" 2D map of mixture **2** centred on the C^6 aromatic carbon site (the all corresponding ^{13}C signals were spectrally discriminated by three resonances). The two doublets of the *meso* compound were arbitrarily chosen as being the two external ones of the ^{2}H 1D spectrum. In this case, the two quadrupolar doublets correlated to the same ^{13}C peak belong to the *meso* (peaks labelled by open and solid squares on the 2D map).

Experimentally, only two ^{13}C signals (122.0 and 122.2 ppm) were observed for C^6 due to the overlap of ^{13}C peaks of the *unlike* and of one of the *like* isomers. Consequently, it wouldn't be possible to assign directly the signals from the analysis of the "D–H–C" 2D map as in Fig. 9. To this end, we would have to record the ^{2}H spectrum of mixture **2** in an achiral mesophase, noted PCBL (or PBG) made by adding equal amount of PCBLL (PBLG) and PCBDL (PBDG), its enantiomer [6]. In this achiral medium, any spectral enantiodiscrimination is eliminated, and hence the magnitude of ^{2}H quadrupolar doublets or the ^{13}C chemical shift values measured in this medium correspond to the algebraic average of values measured in the chiral mesophase. Collapsing of the ^{13}C signals belonging to the *RR* and *SS* compounds should result and so we would obtain a 2D map where two ^{2}H doublets in the F_1 dimension, one for the *meso* and one for the *RR*/*SS* isomers ($|\Delta\nu_Q^{RR,SS}| = 87$ Hz/$|\Delta\nu_Q^{meso}| = 342$ Hz), would be correlated with two ^{13}C peaks of equal intensity in the F_2 dimension. The magnitude of $\Delta\nu_Q$s measured in the achiral mesophase would allow the assignment of the two doublets belonging to the *meso* derivative and *RR*/*SS* isomers.

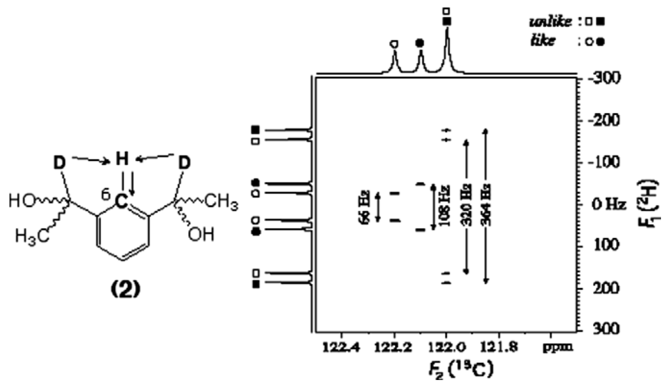

Fig. 9. Simulated 100.3 MHz "D,H,C" 2D spectrum of mixture **2** dissolved in a chiral mesophase where ^2H and ^{13}C signals (aromatic carbon 6) for each stereoisomer are spectrally discriminated. ^2H quadrupolar splittings and ^{13}C chemical shifts used for those simulations are similar to the values measured on experimental ^2H–{^1H} and ^{13}C–{^1H} 1D spectra of mixture **2** dissolved in the PCBLG/$CHCl_3$ phase at 317 K. The parameters τ_{DH}, τ_1, τ_2, τ_3 and τ_{CH}, are equal to 250, 36.5, 35.3, 1.2 and 2.4 ms (i.e. $|^1J_{CH}| = 208$ Hz). The sign of quadrupolar splittings for the *meso* compound and enantiomers are assumed to be the same (positive or negative).

3. Conclusions

This methodological work describes several 2D NMR strategies dedicated to the analysis of ^2H spectra of a mixture of deuterated *u/l* aromatic compounds using weakly ordering chiral oriented solvents. We have designed various homo- and heteronuclear 2D experiments such as the "D(H)$_n$D" or "D(H)$_n$C" correlation experiments (with $n = 1, 2$) towards this goal. Series of experiments on model compounds have demonstrated the efficacy of the various sequences proposed here even if the initial aim was not experimentally reached. These new 2D pulse sequences are based on INEPT-type polarization transfers, but DEPT-type schemes should also induce efficient heteronuclear transfers. We are currently engaged in exploring such an alternative.

Another possible improvement of the sequences proposed here could consist in eliminating H–H strong couplings or reducing the magnitude of H–H couplings between the proton(s) used as relay and other protons in the molecule in order to reduce the dispersion of MQ magnetization through useless protons. This could be performed by introducing multiple-pulse homonuclear decoupling sequences such as "FF-16" or "BLEW-48" sequences in periods where MQ magnetization evolves under the effect of H–H couplings between the proton(s) used as relay and other protons in the molecule [20–23].

4. Experimental

4.1. Synthesis of compounds

The synthesis of mixtures **1** and **2** can be found in Ref. [6], while the compound **3** is commercially available from Isotec Company.

The 2,4,6-trideutero-3-methylphenol, **4**, was prepared using the following procedure. The 3-methylphenol was selectively deuterated to 2,4,6-trideutero-3-methylphenol by repeated exchange in 10% DBr in D_2O under reflux for 10 h. After evaporation of the DBr/D_2O the residue was dissolved in ether and the phenolic hydroxy-group was back exchanged by extraction with H_2O, the ether phase was dried, the solvent evaporated and the deuterated compound was distilled under reduced pressure in a bulb-tube. The degree of deuteration was checked by NMR in $CDCl_3$/TMS and was found better than 96%. Compound **5** was prepared enantiomerically enriched using the asymmetric reduction method developed by Mosher et al. [24].

The description of NMR sample preparation can be found in Ref. [2,3]. Exact composition of each sample is given in Table 1.

4.2. NMR spectroscopy

The 2D experiments were performed on Bruker DRX high-resolution spectrometers at 14.1 T and 9.4 T. The first one is equipped with a 5-mm selective ^2H cryogenic probe. The second one is equipped with a 5-mm four-channel probe (QXO). This probe allows the matching and tuning of the deuterium channel (outer coil), but the ^2H channel (lock) of any probes (dual or broadband) can be used to perform such experiments [9]. The temperature of the sample was controlled by the standard variable temperature unit of the spectrometer and the experiments were performed without sample spinning. All 2D matrices were zero-filled to $1k\ (t_1) \times 2k\ (t_2)$ data points prior to the double Fourier transformation. For all sequences, the full phase cycling is obtained by applying the CYCLOPS procedure to the basic phase cycling given in figure caption, and the quadrature detection in the F_1 dimension uses the TPPI method. All experiments reported here lead to a NMR signal modulated in phase due to the the evolution under the effect of quadrupolar splittings during some of the re- and defocusing periods in the sequences. Hence, 2D contour plots have to be displayed in magnitude mode. In 2D maps, the projections reported correspond to the respective 1D spectra. Other experimental NMR parameters or details are given in the figure captions.

The simulated "D,H,C" spectrum was calculated using NMRSIM (4.3) program included in the TOPSPIN software (1.3) developed by Bruker Biospin. The 2D matrix was made of $512(t_1) \times 1024(t_2)$ data points with $NS = 8$. Neither zero-filling or filtering window were applied prior to the double FT.

Acknowledgements

The authors thank Dr. J.-M. Péchiné for the gift of compound **5**. K.B. and O.L. gratefully thank the CNRS of Gif-sur-Yvette for a financial support, and the MNESR for a PhD grant, respectively.

References

[1] I. Canet, J. Courtieu, A. Loewenstein, A. Meddour, J.-M. Péchiné, Enantiomeric analysis in a polypeptide lyotropic liquid crystal by deuterium NMR, J. Am. Chem. Soc. 117 (1995) 6520–6526.

[2] P. Lesot, M. Sarfati, J. Courtieu, Natural abundance deuterium NMR spectroscopy in polypeptide liquid crystals as a new and incisive means for the enantiodifferentiation of chiral hydrocarbons, Chem. Eur. J. 9 (2003) 1724–1745.

[3] M. Sarfati, P. Lesot, D. Merlet, J. Courtieu, Theoretical and experimental aspects of enantiomeric differentiation using natural abundance multinuclear NMR spectroscopy in polypeptide liquid crystals, Chem. Commun. (2000) 2069–2081, and references therein.

[4] C. Aroulanda, M. Sarfati, J. Courtieu, P. Lesot, Investigation of enantioselectivity of three polypeptide liquid-crystalline solvents using NMR spectroscopy, Enantiomer 6 (2001) 281–287.

[5] A. Meddour, C. Canlet, L. Blanco, J. Courtieu, Diastereomeric shape recognition using NMR spectroscopy in a chiral liquid crystalline solvent, Angew. Chem., Ed. Int. 38 (2001) 2391–2393.

[6] C. Canlet, D. Merlet, P. Lesot, A. Meddour, A. Loewenstein, J. Courtieu, Deuterium NMR stereochemical analysis of *threo–erythro* isomers bearing remote chiral centres in racemic and non-racemic liquid crystalline solvents, Tetrahedron: Asymmetry 11 (2000) 1911–1918.

[7] C. Aroulanda, D. Merlet, J. Courtieu, P. Lesot, NMR experimental evidence of the differentiation of enantiotopic directions in C_s and C_{2v} molecules using partially oriented, chiral media, J. Am. Chem. Soc. 123 (2001) 12059–12066.

[8] H. Villar, F. Guibé, C. Aroulanda, P. Lesot, Investigation of SmI_2 mediated cyclisation process of δ-iodo-α,β-unsaturated esters by deuterium 2D NMR in oriented solvents, Tetrahedron: Asymmetry 13 (2002) 1465–1475.

[9] P. Lesot, M. Sarfati, D. Merlet, B. Ancian, J.W. Emsley, B.A. Timimi, 2D-NMR strategy dedicated to the analysis of perdeuterated enantiomeric solutes in weakly ordered chiral liquid crystals, J. Am. Chem. Soc. 125 (2003) 7689–7695.

[10] E. Lafontaine, J.-M. Péchiné, J. Courtieu, C.L. Mayne, Vizualisation of enantiomers in cholesteric solvents through deuterium NMR, Liquid Crystals 7 (1990) 293–298.

[11] O. Lafon, P. Lesot, Theoretical and experimental investigation of ^{13}C relayed ^{1}H–^{1}H-COSY 2D experiments: applications to the analysis of weakly aligned solutes, J. Magn. Reson. 174 (2005) 254–264.

[12] G.A. Morris, R. Freeman, Enhancement of nuclear magnetic resonance signals by polarization transfer, J. Am. Chem. Soc. 101 (1979) 760–762.

[13] D.M. Doddrell, D.T. Pegg, M.R. Bendall, Distortionless enhancement of NMR signals by polarization transfer, J. Magn. Reson. 48 (1982) 323–327.

[14] J. Keeler, in: Understanding NMR spectroscopy, Wiley, VCH, 2005, p. 223.

[15] M.H. Levitt, in: Spin dynamics, second ed., Wiley, VCH, 2005, p. 459.

[16] A. Bax, D.G. Davis, MLEV-17 two-dimensional homonuclear magnetization transfer spectroscopy, J. Magn. Reson. 65 (1985) 355–360.

[17] P. Lesot, J. Courtieu, D. Merlet, J.W. Emsley, Discrimination and analysis of the NMR spectra of enantiomers dissolved in chiral liquid crystal solvents through 2D correlation spectroscopy, Liquid Crystals 21 (1996) 427–435.

[18] L. Kay, E. Ikura, A. Bax, The design and optimization of complex NMR experiments: Application to a triple-resonance pulse scheme correlating α-proton, amido and ^{15}N chemical shifts in ^{15}N–^{13}C labeled proteins, J. Magn. Reson. 91 (1991) 84–92.

[19] S. Berger, S. Braun, in: 200 and more NMR experiments, Wiley, VCH, 2004.

[20] P. Lesot, J.-M. Ouvrard, B.N. Ouvrard, J. Courtieu, Coherent reduction of dipolar interactions in molecules dissolved in anisotropic media using a new multiple-pulse sequence in a COSY experiment, J. Magn. Reson. A 107 (1994) 141–150.

[21] P. Lesot, J.W. Emsley, J.-M. Ouvrard, E. Curzon, Simplification of ^{19}F NMR spectra of liquid crystalline sample by multiple-pulse COSY experiments, J. Magn. Reson. A 133 (1998) 166–172.

[22] J. Farjon, W. Bermel, C. Griesinger, Resolution enhancement in spectra of natural products dissolved in weakly orienting media with the help of ^{1}H homonuclear dipolar decoupling during acquisition: application to ^{1}H–^{13}C dipolar coupling measurements, J. Magn. Reson. 180 (2006) 72–82.

[23] D.P. Burum, M. Linder, R.R. Ernst, Low power multipulse line narrowing in solid state NMR, J. Magn. Reson. 44 (1981) 173–188.

[24] S. Yamaguchy, H.S. Mosher, Asymmetric reductions with chiral reagents from lithium aluminium hydride and (+)-(2*S*,3*R*)-4-dimethylamino-3-methyl-1,2-diphenyl-2-butanol, J. Org. Chem. 38 (1973) 1870–1871.